Research Article | Vol. 25, No. 9 | 1 May 2017 | OPTICS EXPRESS 10441

Optics EXPRESS

Nonlinear imaging of nanostructures using beams with binary phase modulation

LÉO TURQUET,[1,4] JOONA-PEKKO KAKKO,[2] HUA JIANG,[3] TERO J. ISOTALO,[1] TEPPO HUHTIO,[2] TAPIO NIEMI,[1] ESKO KAUPPINEN,[3] HARRI LIPSANEN,[2] MARTTI KAURANEN[1], AND GODOFREDO BAUTISTA[1,5]

[1]*Laboratory of Photonics, Tampere University of Technology, P.O. Box 692, FI-33101 Tampere, Finland*
[2]*Department of Electronics and Nanoengineering, Aalto University, P.O. Box 13500, FI-00076 Aalto, Finland*
[3]*Department of Applied Physics and Nanomicroscopy Center, Aalto University, P.O. Box 15100, FI-00076 Aalto, Finland*
[4]*leo.turquet@tut.fi*
[5]*godofredo.bautista@tut.fi*

Abstract: We demonstrate nonlinear microscopy of oriented nanowires using excitation beams with binary phase modulation. A simple and intuitive optical scheme comprising a spatial light modulator gives us the possibility to control the phase across an incident Hermite-Gaussian beam of order (1,0) (HG_{10} mode). This technique allows us to gradually vary the spatial distribution of the longitudinal electric fields in the focal volume, as demonstrated by second-harmonic generation from vertically-aligned GaAs nanowires. These results open new opportunities for the full control of polarization in the focal volume to enhance light interaction with nanostructured materials.

OCIS codes: (180.4315) Nonlinear microscopy; (160.4330) Nonlinear optical materials; (060.5060) Phase modulation; (260.5430) Polarization; (070.6120) Spatial light modulators.

References and links

1. G. Bautista and M. Kauranen, "Vector-field nonlinear microscopy of nanostructures," ACS Photonics **3**(8), 1351–1370 (2016).
2. S. Brasselet, "Polarization-resolved nonlinear microscopy: application to structural molecular and biological imaging," Adv. Opt. Photonics **3**(3), 205–271 (2011).
3. R. W. Boyd, *Nonlinear Optics* (Academic, 2008).
4. B. Richards and E. Wolf, "Electromagnetic diffraction in optical systems. II. Structure of the image field in an aplanatic system," Proc. R. Soc. Lond. A Math. Phys. Sci. **253**(1274), 358–379 (1959).
5. L. Novotny and B. Hecht, *Principles of Nano-Optics* (Cambridge University, 2012).
6. S. Carrasco, B. E. A. Saleh, M. C. Teich, and J. T. Fourkas, "Second- and third-harmonic generation with vector Gaussian beams," J. Opt. Soc. Am. B **23**(10), 2134–2141 (2006).
7. M. J. Huttunen, J. Mäkitalo, G. Bautista, and M. Kauranen, "Multipolar second-harmonic emission with focused Gaussian beams," New J. Phys. **14**(11), 113005 (2012).
8. E. Yew and C. Sheppard, "Effects of axial field components on second harmonic generation microscopy," Opt. Express **14**(3), 1167–1174 (2006).
9. A. A. Asatryan, C. J. R. Sheppard, and C. M. de Sterke, "Vector treatment of second-harmonic generation produced by tightly focused vignetted Gaussian beams," J. Opt. Soc. Am. B **21**(12), 2206–2212 (2004).
10. Q. Zhan, "Cylindrical vector beams: from mathematical concepts to applications," Adv. Opt. Photonics **1**(1), 1–57 (2009).
11. T. G. Brown, "Chapter 2 - Unconventional polarization states: beam propagation, focusing, and imaging," Prog. Opt. **56**, 81–129 (2011).
12. T. Züchner, A. V. Failla, and A. J. Meixner, "Light microscopy with doughnut modes: a concept to detect, characterize, and manipulate individual nanoobjects," Angew. Chem. Int. Ed. Engl. **50**(23), 5274–5293 (2011).
13. H. Kogelnik and T. Li, "Laser beams and resonators," Appl. Opt. **5**(10), 1550–1567 (1966).
14. K. S. Youngworth and T. G. Brown, "Inhomogenous polarization in scanning optical microscopy," Proc. SPIE **3919**, 75–85 (2000).
15. R. Dorn, S. Quabis, and G. Leuchs, "Sharper focus for a radially polarized light beam," Phys. Rev. Lett. **91**(23), 233901 (2003).
16. L. Novotny, M. R. Beversluis, K. S. Youngworth, and T. G. Brown, "Longitudinal field modes probed by single

#287663 https://doi.org/10.1364/OE.25.010441
Journal © 2017 Received 1 Mar 2017; revised 16 Apr 2017; accepted 17 Apr 2017; published 26 Apr 2017

Optics EXPRESS

molecules," Phys. Rev. Lett. **86**(23), 5251–5254 (2001).
17. M. Kasperczyk, S. Person, D. Ananias, L. D. Carlos, and L. Novotny, "Excitation of magnetic dipole transitions at optical frequencies," Phys. Rev. Lett. **114**(16), 163903 (2015).
18. A. V. Failla, H. Qian, H. Qian, A. Hartschuh, and A. J. Meixner, "Orientational imaging of subwavelength Au particles with higher order laser modes," Nano Lett. **6**(7), 1374–1378 (2006).
19. K. Yoshiki, K. Ryosuke, M. Hashimoto, N. Hashimoto, and T. Araki, "Second-harmonic-generation microscope using eight-segment polarization-mode converter to observe three-dimensional molecular orientation," Opt. Lett. **32**(12), 1680–1682 (2007).
20. E. Y. S. Yew and C. J. R. Sheppard, "Second harmonic generation polarization microscopy with tightly focused linearly and radially polarized beams," Opt. Commun. **275**(2), 453–457 (2007).
21. G. Bautista, M. J. Huttunen, J. Mäkitalo, J. M. Kontio, J. Simonen, and M. Kauranen, "Second-harmonic generation imaging of metal nano-objects with cylindrical vector beams," Nano Lett. **12**(6), 3207–3212 (2012).
22. M. J. Huttunen, K. Lindfors, D. Andriano, J. Mäkitalo, G. Bautista, M. Lippitz, and M. Kauranen, "Three-dimensional winged nanocone optical antennas," Opt. Lett. **39**(12), 3686–3689 (2014).
23. G. Bautista, M. J. Huttunen, J. M. Kontio, J. Simonen, and M. Kauranen, "Third- and second-harmonic generation microscopy of individual metal nanocones using cylindrical vector beams," Opt. Express **21**(19), 21918–21923 (2013).
24. P. Reichenbach, A. Horneber, D. A. Gollmer, A. Hille, J. Mihaljevic, C. Schäfer, D. P. Kern, A. J. Meixner, D. Zhang, M. Fleischer, and L. M. Eng, "Nonlinear optical point light sources through field enhancement at metallic nanocones," Opt. Express **22**(13), 15484–15501 (2014).
25. X. Li, T.-H. Lan, C.-H. Tien, and M. Gu, "Three-dimensional orientation-unlimited polarization encryption by a single optically configured vectorial beam," Nat. Commun. **3**, 998 (2012).
26. F. Lu, W. Zheng, and Z. Huang, "Coherent anti-Stokes Raman scattering microscopy using tightly focused radially polarized light," Opt. Lett. **34**(12), 1870–1872 (2009).
27. W. Han, Y. Yang, W. Cheng, and Q. Zhan, "Vectorial optical field generator for the creation of arbitrarily complex fields," Opt. Express **21**(18), 20692–20706 (2013).
28. M. Comstock, V. Lozovoy, I. Pastirk, and M. Dantus, "Multiphoton intrapulse interference 6; binary phase shaping," Opt. Express **12**(6), 1061–1066 (2004).
29. V. V. Lozovoy, B. Xu, J. C. Shane, and M. Dantus, "Selective nonlinear optical excitation with pulses shaped by pseudorandom Galois fields," Phys. Rev. A **74**(4), 041805 (2006).
30. P. J. Wrzesinski, D. Pestov, V. V. Lozovoy, B. Xu, S. Roy, J. R. Gord, and M. Dantus, "Binary phase shaping for selective single-beam CARS spectroscopy and imaging of gas-phase molecules," J. Raman Spectrosc. **42**(3), 393–398 (2011).
31. B. Li, Y. Xu, H. Zhu, Q. Lin, L. An, F. Lin, and Y. Li, "Spectral compression and modulation of second harmonic generation by Fresnel-inspired binary phase shaping," J. Opt. Soc. Am. B **31**(10), 2511–2515 (2014).
32. H. Wang, L. Shi, B. Lukyanchuk, C. Sheppard, and C. T. Chong, "Creation of a needle of longitudinally polarized light in vacuum using binary optics," Nat. Photonics **2**(8), 501–505 (2008).
33. H. Guo, X. Weng, M. Jiang, Y. Zhao, G. Sui, Q. Hu, Y. Wang, and S. Zhuang, "Tight focusing of a higher-order radially polarized beam transmitting through multi-zone binary phase pupil filters," Opt. Express **21**(5), 5363–5372 (2013).
34. G. Bautista, J. Mäkitalo, Y. Chen, V. Dhaka, M. Grasso, L. Karvonen, H. Jiang, M. J. Huttunen, T. Huhtio, H. Lipsanen, and M. Kauranen, "Second-harmonic generation imaging of semiconductor nanowires with focused vector beams," Nano Lett. **15**(3), 1564–1569 (2015).
35. L. Turquet, J.-P. Kakko, X. Zang, L. Naskali, L. Karvonen, H. Jiang, T. Huhtio, E. Kauppinen, H. Lipsanen, M. Kauranen, and G. Bautista, "Tailorable second-harmonic generation from an individual nanowire using spatially phase-shaped beams," Laser Photonics Rev. **11**(1), 1600175 (2017).
36. J.-P. Kakko, T. Haggrén, V. Dhaka, T. Huhtio, A. Peltonen, H. Jiang, E. Kauppinen, and H. Lipsanen, "Fabrication of dual-type nanowire arrays on a single substrate," Nano Lett. **15**(3), 1679–1683 (2015).
37. X. Xun and R. W. Cohn, "Phase calibration of spatially nonuniform spatial light modulators," Appl. Opt. **43**(35), 6400–6406 (2004).
38. A. Bouhelier, M. Beversluis, A. Hartschuh, and L. Novotny, "Near-field second-harmonic generation induced by local field enhancement," Phys. Rev. Lett. **90**(1), 013903 (2003).
39. L. Novotny, E. J. Sánchez, and X. Sunney Xie, "Near-field optical imaging using metal tips illuminated by higher-order Hermite-Gaussian beams," Ultramicroscopy **71**(1–4), 21–29 (1998).
40. Y. Kozawa and S. Sato, "Optical trapping of micrometer-sized dielectric particles by cylindrical vector beams," Opt. Express **18**(10), 10828–10833 (2010).

1. Introduction

The state of polarization of an excitation beam is usually determined by the local amplitude and relative phase of its transverse optical field components in the far field. For the past decade, it has been shown that the polarization of light is an important parameter to control when performing coherent nonlinear imaging of nano-objects [1,2]. The contrast achieved in nonlinear imaging depends mainly on the intrinsic properties of the specimen [3].

Optics EXPRESS

Importantly, when a transversely polarized field is focused, the focal volume also contains longitudinal field components, i.e., the three-dimensional (3D) electric field strongly depends on the polarization of the incident beam and the focusing parameters [4,5]. As the nonlinear responses are tensorial in nature, the 3D optical fields at the beam focus are expected to strongly modify the overall nonlinear signals [1–3,6–9].

Recently, beams with spatially nonuniform states of polarizations [10–12] have given rise to new opportunities for nonlinear microscopy [1]. Radial and azimuthal polarizations as well as their derivatives are well-known examples of these beams [13]. Due to the unique local polarization distributions of such beams, they give rise to very special 3D field distributions when tightly focused [5,14,15]. For instance, radial and azimuthal polarizations can be used to unambiguously excite oriented molecules and nanostructures [16–26]. Even though the creation of such beams is now well established [10–12], their shaping in space and time often involves cumbersome optical setups [25,27]. A simple way to reduce this complexity is to utilize binary shaping of the local phase of the beams, e.g., 0 and π. Previously, binary phase shapes have been utilized to increase the excitation selectivity in a variety of spectroscopy techniques [28–31] and to decrease the spot size of high-order optical beams [32,33]. To the best of our knowledge, binary phase shaping has not yet been applied to control the focal field distributions and resulting effects in driving the nonlinear emission from nanostructures.

Here, we demonstrate precise and on-demand control of the strength and spatial distribution of the longitudinal electric component of the focal field using a programmable optical setup based on binary phase levels. We present a simple scheme which uses a phase-only spatial light modulator (SLM) that allows to modify the phase of an incoming HG_{10} mode. By applying π-phase jumps with varying spatial coverages, we demonstrate the tailoring of the focal fields and hence of second-harmonic generation (SHG) from vertically-oriented GaAs nanowires.

2. Materials and methods

Previously, we have shown that vertically-aligned GaAs nanowires are excited preferentially by longitudinal fields [34]. More recently, we have shown that such nanowires and SHG can be used as a nanoscale platform to evaluate the strength and spatial distribution of longitudinal electric fields [35]. In our previous work, the focal fields were tailored by applying local phase delays on one part of a HG_{10} mode. In the present work, we use identical nanowires to demonstrate precise control of the longitudinal field for tailoring SHG using a simple scheme involving only π-phase jumps.

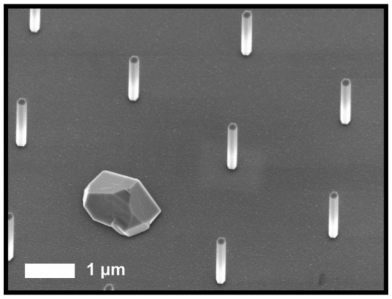

Fig. 1. SEM image of typical GaAs nanowires used in the experiment.

Our GaAs nanowires were grown vertically along the [111] direction on a GaAs substrate using selective-area metallo-organic vapour phase epitaxy. The nanowires showed a zinc-blende structure with some twin defects. Further details regarding the fabrication can be found in our previous works [35,36]. To prevent possible coupling between the neighboring nanowires, we excited nanowires that were equally distributed on an array with a 2.3 µm pitch. The nanowires have a diameter of 50 nm and a length of 2.5 µm based on scanning

Optics EXPRESS

electron microscopy (SEM) measurements. Nanowires similar to our sample are shown in Fig. 1.

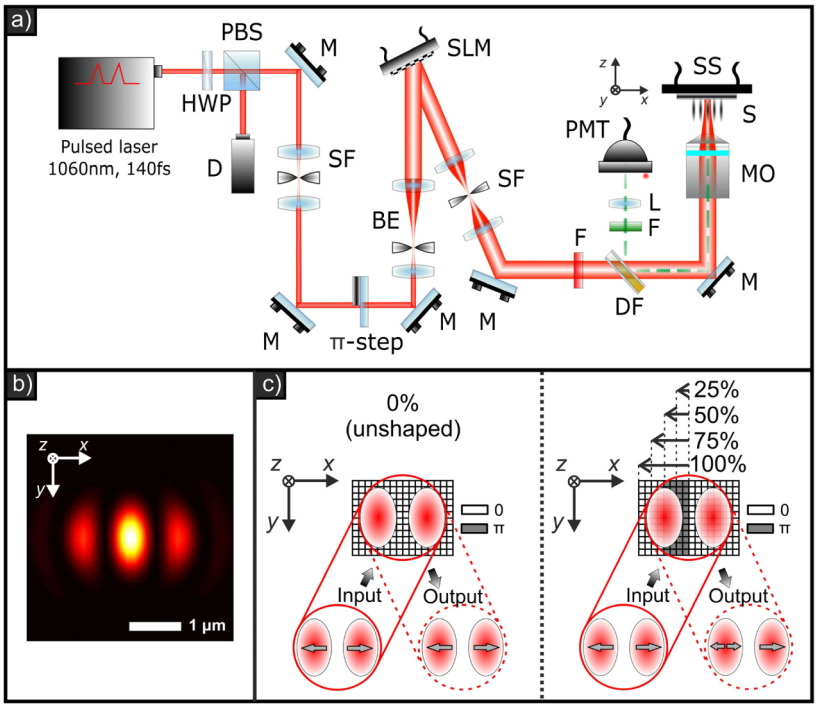

Fig. 2. a) Schematic of the optical setup (HWP: half-wave plate, PBS: polarizing beamsplitter, M: mirror, D: beam dump, SF: spatial filter, BE: beam expander, F: filter, DF: dichroic filter, L: lens, PMT: photomultiplier tube, MO: microscope objective, NA = 0.8, 50 × , S: sample, SS: stage scanner). Red lines: path of fundamental excitation beam (1060nm), green dashed lines: path of SHG signal. b) Calculated spatial distribution of longitudinal electric field of tightly focused linearly-polarized HG_{10} mode at the focal plane under our experiment settings (excitation wavelength of 1060 nm, NA of 0.8). The polarization of the incident HG_{10} mode is along *x*. The data were obtained using the angular spectrum approach [5]. c) Spatial intensity distribution of both the incoming and reflected HG_{10} mode off from the SLM when unshaped (0%) and for different π coverages (25%, 50%, 75%, and 100%). The additional π-phase delay applied on the left lobe starts from the center of the SLM aperture. The coverage increases from the center to the left.

Our optical setup is based on a point-scanning nonlinear microscope with a phase-shaping scheme on the illumination side [Fig. 2(a)]. The optical path is similar to the one presented in our previous work with differences in the phase-shaping process [35]. Before entering the microscope objective, the excitation beam was first manipulated to create a linearly-polarized HG_{10} mode. For this, the HG_{00} output beam of the laser was directed to a π-phase step element, which contains a 560-nm thick layer of SiN on one half of a glass window, in order to produce a linearly *x*-polarized HG_{10} mode after spatial Fourier filtering. It is important to note that other techniques exist to create an HG_{10} mode, but the chosen technique is the most practical. We justify the use of an *x*-polarized HG_{10} mode for two reasons. First, it shows a strong on-axis longitudinal electric field at the focus [Fig. 2(b)], a required feature for efficiently exciting vertically-aligned nanowires [35]. Second, its spatial distribution and polarization in the far field make it suitable for phase-shaping using a SLM. Thus, the resulting HG_{10} mode was steered toward the aperture of a computer-controlled reflective-type phase-only SLM (Hamamatsu X10468-07). This model shows a very high fill factor of 98%, maximizing the phase-shaping efficiency. The SLM provides a high degree of flexibility as it eliminates the need for a variety of diffractive optical elements for phase control.

https://doi.org/10.1364/OE.25.010441

Optics EXPRESS

Figure 2(c) shows the phase-shaping scheme utilized in this work. The aperture of the SLM was numerically divided into two identical sub-windows. The lobes of the incident HG_{10} mode were assigned to impinge symmetrically on the two sub-windows. After phase calibration at our fundamental wavelength of 1060 nm and careful alignment, we applied a π-phase jump for different coverages on one lobe of the HG_{10} mode, starting from the center of the SLM aperture. We chose to start increasing the phase coverage from the center to get rid of the possible nonuniform phase response often observed at the edges of an SLM display [37]. The reflected phase-shaped beam was then spatially-filtered and steered toward the microscope objective [numerical aperture (NA) of 0.8]. The HG_{10} mode experiencing no additional phase delay from the SLM, the 0% coverage, is defined as "unshaped". For each coverage (0%, 25%, 50%, 75%, and 100%), we collected a two-dimensional scanning microscopy image of the sample.

The strength of this technique relies on its simple design and understanding. On one hand, the *x*-polarized HG_{10} mode is composed of two intensity lobes in the far field. When strongly focused, its longitudinal component at the focus forms a three-lobe pattern with a strong peak on the optical axis [Fig. 2(b)] [35,38,39]. This strong longitudinal field on the axis arises from the two lobes of the HG_{10} mode oscillating with opposite phase in the far field [Fig. 2(c)]. On the other hand, a tightly focused *x*-polarized HG_{00} shows a longitudinal field composed of two lobes at the focus [4]. By introducing a π-delay with increasing coverage on one lobe of the HG_{10} mode using the SLM, we aim to gradually make the two lobes oscillate in phase and approach an ordinary *x*-polarized beam distribution, therefore switching from strong to weak longitudinal field on the optical axis at the focus of the microscope objective.

3. Results and discussion

It is known that the strong SHG signals originate from GaAs nanowires and not from the substrate [34]. However, prior to longitudinal field tailoring, we had to verify that variations in SHG signals originate only from pure phase shaping of the HG_{10} mode.

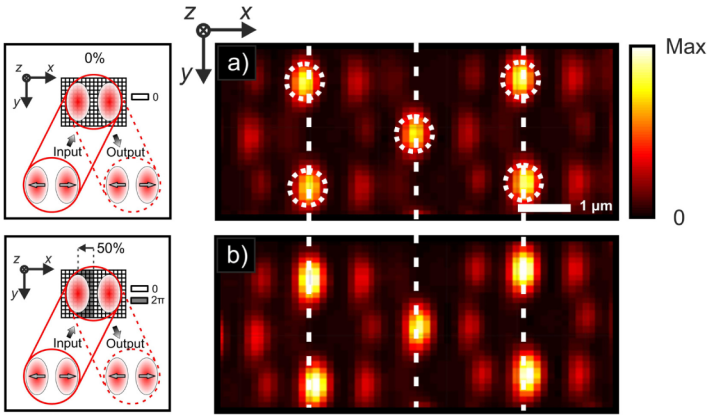

Fig. 3. SHG intensity maps of five vertically-aligned GaAs nanowires using a) an unshaped HG_{10} mode (0% coverage) and b) by applying an additional 2π delay with a 50% coverage on one lobe of the HG_{10} mode. The input power is 1 mW and the pixel dwell time is 50 ms. Respective phase distributions on the SLM are shown for clarity. White dash circles represent the location of the nanowires extended by white dash lines for guidelines to the eye.

Figure 3(a) shows the SHG intensity maps of nanowires excited with an unshaped HG_{10} mode. We observe the clear three-lobe distribution resembling the longitudinal field of a tightly focused HG_{10} mode, with a maximum at the location of the nanowire, which is consistent with previous works [35,38,39]. The possible asymmetry in term of intensity between the side lobes is attributed to small imperfections of the π-phase element, showing a slightly (30 nm) thick SiN layer. Figure 3(b) shows then the SHG intensity map of the

https://doi.org/10.1364/OE.25.010441

Optics EXPRESS

nanowires excited using an HG_{10} mode, with one lobe experiencing an additional 2π delay for a coverage of 50%. By applying a 2π delay, we should recover the far field configuration of an unshaped HG_{10} mode and thus observe the same SHG image features. As expected, results are similar and still show a three-lobe distribution centered at the nanowire location. The phase coverage used here does not play a role as a 2π delay is used. Any other coverage could have been used, leading to the same results. By this, we have thus demonstrated that the beam manipulation is free from any other factors but pure phase shaping and that phase jumps applied in the middle of one lobe do not affect the propagation of the beam toward the microscope objective.

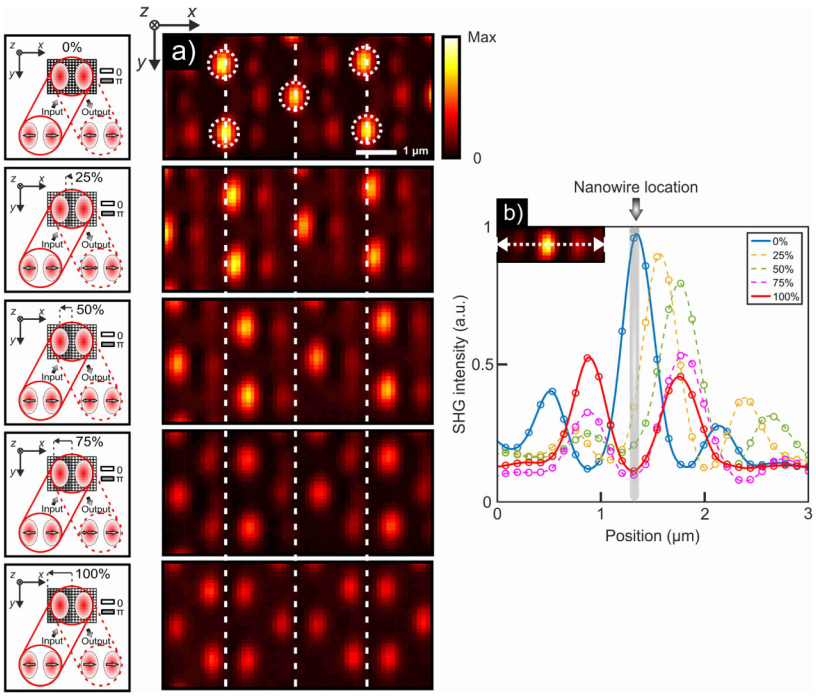

Fig. 4. a) SHG intensity maps of five vertically-aligned GaAs nanowires for different π coverages on one lobe of the HG_{10} mode with an additional phase delay starting from the center of the SLM aperture (0%, 25%, 50%, 75%, and 100% as inset). The input power is 1 mW and the pixel dwell time is 50 ms. White dash circles represent the location of the nanowires extended by white dash lines for guidelines to the eye. b) SHG intensity profiles taken for the different coverages and averaged over three line cuts centered on the nanowire as specified on the inset. The location of the nanowire is specified for clarity.

We then implemented the binary phase shaping scheme. Starting from the center of the SLM aperture to the left edge of the SLM aperture, the additional π-phase delay was applied over 0%, 25%, 50%, 75%, and 100% of one lobe of the input HG_{10} mode. For each coverage, the SHG response from a raster scan of the nanowires was collected and can be seen on Fig. 4(a). For 0%, that is to say no delay applied, we observe the three-lobe distribution centered at the location of the nanowire. Then, and as already observed in our previous work, applying an additional π delay over 100% of one of the HG_{10} lobe generates a longitudinal field resembling that of a focused linearly *x*-polarized Gaussian beam. In this configuration, the two lobes of the HG_{10} mode oscillate in phase leading to a longitudinal field composed of two off-axis lobes at the focus. The results for 0% and 100% coverages are thus consistent with our previous findings [35]. For increasing intermediate coverages, however, we observe a gradual change in the intensity and distribution of the SHG response from the nanowires. This behavior allows us to see how the longitudinal field slowly shifts from a three to a two-lobe

https://doi.org/10.1364/OE.25.010441

Optics EXPRESS

distribution. Increasing the π coverage leads to a gradual shift of the center lobe to the right in this case. As the π-coverage in one lobe of the HG_{10} mode is increased, i.e., along the incident polarization and from 0% to 100% with respect to the center of the SLM aperture or beam, the resulting beam at the focus increasingly becomes linearly-polarized. Thus, as the π-coverage increases, the longitudinal electric field component at the off-axis (on-axis) positions of the focal plane increases (decreases). Due to spatial symmetry of the incident beam, the application of the binary phase-shaping scheme on the other lobe of the HG_{10} mode will result in an opposite spatial shift.

In order to better understand the variations of the longitudinal field with respect to the nanowire location and the delay applied, we focused on a single nanowire and plotted the line profiles for all π coverages. The results can be seen on Fig. 4(b). Each line profile is the result of the mean over three parallel line cuts centered at the peak intensity for each coverage, as specified on the inset of Fig. 4(b). It can be seen that the center peak shifts to the right of the nanowire for increasing coverage. Finally, the longitudinal field takes the form of a two-lobe intensity distribution with minimum intensity at the location of the nanowire when one of the HG_{10} lobes is fully π delayed. If we consider the precise location of the nanowire, we clearly observe a decrease in SHG intensity, that is to say a decrease in the strength of the longitudinal field. The gradually varying SHG intensity patterns represent then the transition between a strong to a weak longitudinal field on the optical axis at the focus. This behavior confirms and justifies the use of our technique for controlling precisely the strength of the longitudinal field at focus. Alternatively, this technique also allows a precise tuning of the longitudinal field distribution without mechanical intervention.

Although gradual spatial shifts of the longitudinal electric fields can be also observed in a lobe of a HG_{10} mode that is partially encoded (i.e., with coverages of 25%, 50% and 75%) with phase delays from 0 to 2π, the resulting images at the different phase delays are expected to exhibit low contrast. This issue becomes even more problematic in coherent nonlinear microscopy, where the signal levels are already very weak. By using only binary phase shaping (0 and π), we have shown that the image contrast at different coverages remains high [Fig. 4]. Binary phase shaping at different coverages also makes the setups simpler because it does not require the full phase range of the SLM, which requires precise calibration beforehand. This is important for SLM-based nonlinear microscopy where the operable excitation wavelengths remain limited [1].

4. Conclusion and outlook

Through simple binary phase shaping, we have demonstrated precise and on-demand control of longitudinal fields at the focus of a beam. The SLM provides versatility and practicality to this optical scheme that dramatically simplify the beam shaping operation for the control of the longitudinal field in the focal volume. This work shows direct application to the tailoring of nonlinear responses of vertically-aligned nanostructures and sets the first steps toward the full control of polarization in 3D for various microscopy applications. These applications include improved light coupling into nano-objects and molecular systems for contrast enhancement and 3D orientation characterization. Future improvement and plans include the implementation of similar schemes for shaping the focal field components of other high-order beams therefore being able to fully engineer the focal field distribution in 3D. Such a system would be beneficial for various light-matter phenomena where focal field control is crucial. The latter include the collection of highly selective information in optical microscopy of single molecules [16], breakthroughs in optical trapping [40] and selective excitation of nano-objects [36].

Optics EXPRESS

Funding

Academy of Finland (267847, 287651); Investment funding of Tampere University of Technology (84010); MOPPI project of Aalto Energy Efficiency Research Programme; TEKES FiDiPro NP Nano project.

Acknowledgments

L.T. acknowledges the financial support from the Graduate School of Tampere University of Technology. Nanowire fabrication was performed at the Micronova Nanofabrication Centre of Aalto University. This work made use of the Aalto University Nanomicroscopy Center premises. This work was performed in the context of the European COST Action MP1302 Nanospectroscopy.